Regular Article

Variability in the power-law distributions of rupture events

How and why does b-value change

D. Amitrano[a]

ISTerre, CNRS-University of Grenoble, France

Abstract. Rupture events, as the propagation of cracks or the sliding along faults, associated with the deformation of brittle materials are observed to obey power-law distributions. This is verified at scales ranging from laboratory samples to the Earth's crust, for various materials and under various loading modes. Besides the claim that this is a universal characteristic of the deformation of heterogeneous media, spatial and temporal variations are observed in the exponent and tail-shape. These have considerable implications for the ability and the reliability of forecasting large events from smaller ones. There is a growing interest in identifying the factors responsible for these variations. In this work, we first present observations at various scales (laboratory tests, field experiments, landslides, mining induced seismicity, crustal Earthquakes) showing that substantial variations exist in both the slope and the tail-shape of the rupture event size distribution. This review allows us to identify potential explanations for these variations (incorrect statistical methods, heterogeneity, stress, brittle/ductile transition, finite size effects, proximity to the failure). A possible link with the critical point theory is also drawn showing that it is able to explain a part of the observed variations considering the distance to the critical point. Using numerical simulations of progressive failure we investigate the role of mechanical properties on the power-law distributions. The results of simulations agree with the critical point theory for various macroscopic behaviors ranging from ductility to brittleness providing a unified framework for the understanding of power-law variability observed in rupture phenomena.

1 Introduction

The deformation of brittle materials is associated with damage (i.e. micro-cracks nucleation and propagation) and friction (i.e. sliding on preexisting cracks or geological faults). These processes occur by the accumulation of discrete events of size spreading over several orders of magnitude. This is observed at scales varying from that of

---

[a] *Present address:* ISTerre, University J. Fourier, Grenoble, BP. 53, 38041 Grenoble Cedex 9, France.

laboratory samples to that of the Earth's crust, including underground excavations, quarries, cliffs, landslides and volcanoes. Scaling invariance is observed for temporal (e.g. the distribution of waiting time), spatial (e.g. fractal structure of the rupture) and size distributions, displaying the complexity of the rupture dynamics. Here we focus on the ubiquitous observation that the size distribution of the rupture events obeys a power-law characterized by its exponent, called *b*-value in the Earth sciences field. Despite the fact that the mean value of this exponent is robustly observed to be near 1 for earthquakes, substantial variations exist in both the slope (e.g. [39]) and the shape of the distribution for largest events, i.e. the tail-shape (e.g. [29]) of the rupture event size distribution. Since the early works of Mogi [32] and Scholz [42] on brittle rocks, there is a constant effort to understand the origins of these fluctuations and whether material properties and mechanical loading conditions are able to explain them.

The dynamics of fracturation and damage during mechanical loading usually displays a power-law distribution of rupture event sizes.

$$N(> s) = c.s^{-\beta} \tag{1}$$

where s is a measure of the rupture event size, $N(> s)$ is the number of events with size larger than s, c and β are constants. $N(> s)$ is the empirical cumulative distribution function, *cdf*. The frequency size relationship can also be examined using the probability density function, *pdf*, which is obtained by derivating the cumulative distribution function. In the case of power-law, the exponent of the *pdf* equals $-\beta-1$.

$$p(s) = c'.s^{-\beta-1} \tag{2}$$

In numerical simulations, the rupture event size can be estimated by the number of broken bonds during an avalanche for fracture models, or by the area of a slip zone in friction models. In laboratory experiments, when using acoustic emission (AE) monitoring for observing the damage dynamics, s can be estimated by the signal maximum amplitude A or energy E. The absolute value of the β exponent depends on the metrics used for characterizing the event size s. In AE monitoring, theoretical considerations, well verified empirically allows us to consider that E scales with A^2 [27], so that both $N(> A)$ and $N(> E)$ obey power-law,

$$N(> A) = c_A.A^{-\beta_A} \tag{3}$$

$$N(> E) = c_E.E^{-\beta_E} \tag{4}$$

but the exponents will be different in the two cases, with the scaling relationship $\beta_A = 2\beta_E$.

In a log-log representation, such power-law distributions appear linear and exponent β is given by the slope of the line.

$$\log N(> s) = \log c - \beta.\log s \tag{5}$$

This distribution exhibits remarkable similarity with the Gutenberg-Richter empirical relationship observed for earthquakes [19].

$$\log N(> M) = a - bM \tag{6}$$

Where $N(> M)$ is the number of earthquakes with a magnitude larger than M. The magnitude M is theoretically and empirically related to the energy E released by the seismic rupture [20,43]
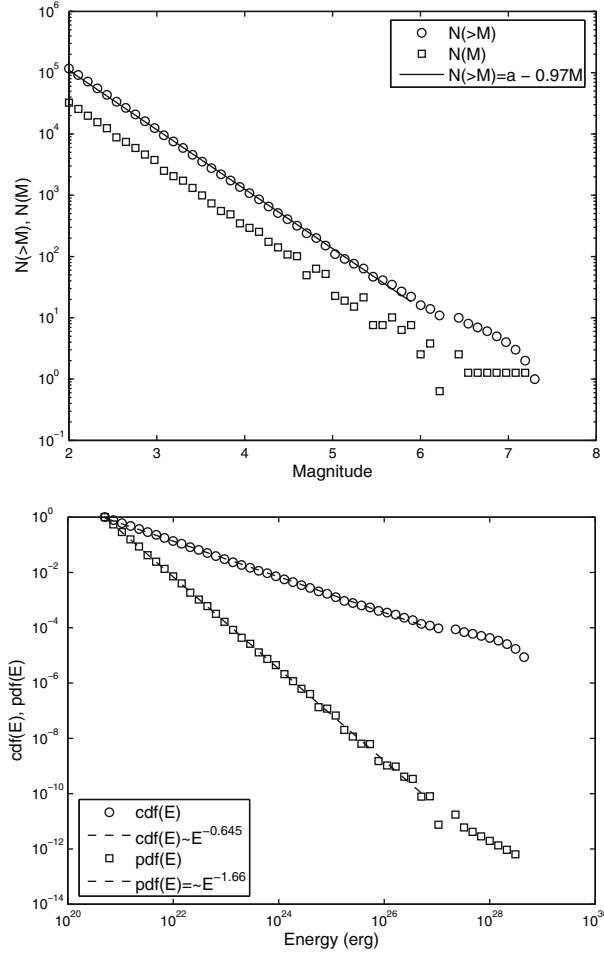
$$M = \frac{2}{3}\log E - 11.8 \tag{7}$$

Fig. 1. Earthquake magnitude distribution in California from 1990 to 2010 (extract from the ANSS catalog). Top: cumulative $N(> M)$ and discrete $N(M)$ distribution of magnitude. Bottom: cumulative distribution *cdf* and probability density functions *pdf* of the Energy. The *pdf* is normalized for plotting convenience.

where E is in ergs. So the values of b, β_A and β_E are linearly related as follows: $b = \frac{3}{2}\beta_E = \frac{3}{4}\beta_A$. Figure 1 shows an example of magnitude and energy distributions observed for California earthquakes with the corresponding exponents. The former relation between the exponents is empirically well verified.

As power-laws indicate scale invariance and because of the similarities in the underlying physics, AE of rocks observed in the laboratory has been considered as a small-scale model of the seismicity of the Earth's crust [42]. Observations of both earthquakes and AE show variations of the *b*-value in time and space domains. The purpose of this work is to identify possible origins of these variations and to provide a physical model able to explain them. The paper is organized as follows:

i) A review of laboratory and field observations of *b*-value variations and outcomes of numerical models able to produce power-law distributions of rupture events, providing a short list of potential explanations of the *b*-value variations.
ii) Detailed analysis of each potential explanation and of their effect on *b*-value.

iii) Numerical modeling showing the effect of the mechanical properties on both the power-law exponent and the tail-shape. Analysis of the agreement with critical point theory.

2 Observed variations in the power-law distributions of rupture events

2.1 Experimental and Field observations

Mogi [32], suggested that the b-value depends on the material heterogeneity, a low heterogeneity leading to a low exponent. Scholz [42] observed that the b-value decreased before the stress peak of rock specimens compressed in the laboratory and argued for a negative correlation between b-value and stress. The relationship between the b-value and the fractal dimension D of AE source locations has also been investigated in the laboratory [28] and showed a decrease of b-value in conjunction with the strain localization, i.e. to a decrease of D-value. These patterns have been observed essentially for brittle rocks (e.g. [22,25]) and for other heterogeneous materials such as chipboard, fiberglass [18] or paper [40] providing arguments for the existence of a relationship between the b-value decrease to the progressive spatial clustering of the damage.

Temporal fluctuations of the b-value have also been observed for earthquakes leading some authors to consider the b-value decrease as a precursor to major earthquakes being considered as macro-failure events [26,48,53,54]. Observations of the seismicity emitted by a rock cliff before a collapse revealed that such a decrease of the b-value was associated with a power-law acceleration of the event rate and of the released energy rate [7]. Considering that such a pattern fits with the critical point theory, the authors suggested that the apparent b-value decrease could be induced by a cut-off of increasing size as the failure approaches rather than by a real change of the power-law exponent.

For brittle rocks, the b-value has been reported to depend on the mechanical loading conditions, i.e. type of faulting for Earthquakes [45], the confining pressure [3], or the roughness of sliding surfaces [41] in the laboratory. All these observations agree with a dependence of the b-value on friction and/or mean stress. The distinction between these two factors remains difficult because they are observed to be correlated [3], as friction decrease when the confining pressure increases [23].

Spatial variations of the b-value have been studied by calculating this parameter on small areas for tracking spatial variations of either the stress or the mechanical properties of the Earth's crust (e.g. [33,60,61]). A decrease of the b-value with increasing depth has been observed for earthquakes in California [16,34]. Similar depth dependence has been observed in the western Alps [51] and for induced seismicity related to Aswan Lake in Egypt [30] indicating a possible relationship between b-value and the mean stress and/or the brittle/ductile transition. Schorlemner et al [44] observed that the M=6 Parkfield earthquake fits well an area of particularly low b-value, suggesting that this parameter could be used to identify areas prone to the failure.

A few studies display variations in the shape of the distribution tails, showing that the power-law trend is not always respected for the largest events of the catalogue (e.g. [29]). The distribution tail can be characterized alternatively by a lack (cut-off e.g. [51]) or by an excess (oversizing e.g. [10]) of large events compared with the power-law trend. This discrepancy with the power-law trend is of major importance regarding the ability to estimate the probability of the largest events by extrapolation of the observed distribution for the smaller ones.

2.2 Numerical simulations

Many studies used numerical simulation in order to recover power-law distributions of failure events (see [2] for a review). A common outcome of these simulations is that power-law distributions emerge spontaneously from elastic interaction within heterogeneous media [4]. Early models based on cellular automata simulating the behavior of a network of sliding blocks connected by springs [11,13,35] aimed to reproduce the behavior of a fault. These models reach a metastable state characterized by a power-law distribution of avalanches with an exponent remaining constant. The value of the exponent may change depending on the rules of interaction and of the non-conservative part of the energy balance.

Fiber bundle and lattice solids models, with of without electrical-mechanical analogy, have been extensively used for characterising the emergence of power-law in rupture phenomena, particularly as the macro-failure is approached (e.g. [38,62,63]). Due to its numerical simplicity, this type of model allowed the authors to investigate the behavior of large size models and in particular to identify the role of the finite size of the system and of the distance to the critical point on the emergence of power-law distributions. They showed in particular that power-law distributions of rupture avalanches are fully developed only in the vicinity of the critical point, i.e. the macrofailure, as described in critical point theory [49]. Variations in the power-law shape and tail are shown to be related to the presence of an exponential cut-off that depends on the finite size of the model and diverges as the critical point is approached. The finite rate of the loading has also been proposed to induce a cut-off of the power-law distribution for largest size events [36,39]. The evoked mechanism is that the loading rate should be infinitely small, or small enough, for allowing the long range interaction that permits the emergence of avalanches at all scales. In the case of a too fast loading, viscous dissipation could contradict the full range elastic interaction, limiting the emergence of largest rupture events. Departure from pure power-law may also originate from avalanches that overlap.

Models including more realistic rules of stress redistribution, energy dissipation, strain softening or hardening (e.g. [9,15]) allow investigation of the conditions of appearance of cut-off or characteristic size failure events. More complex models including tensorial description of the stress state have been proposed [3,6,52] that simulate both the progressive damage of brittle solids, the damage localization process and, for some of them, the power-law distributions of rupture events. This type of model has been shown to produce critical behavior associated with damage localization [17]. The tensorial description of the elastic interaction allowed to draw the connection between the power-law distributions of rupture and the scale invariance of the strain field. This argues for the importance of long range correlation in the emergence of power-law distribution of rupture events.

2.3 Potential explanations for power-law variations

2.3.1 Incorrect statistical methods

The main statistical bias is obviously related to the number of events, i.e. the size of the catalogue, used for calculating the exponent of the power-law distribution. Many studies, essentially field works, estimated the b-value on samples as small as a few hundred events. This is generally due to the difficulty of reaching a large number of well-identified seismic events in certain field conditions. Systematic tests based on random sampling from power-law distribution [37] have shown that the confidence of the b-value estimated by least squares regression decreases as the sample size increases. It becomes lower than 0.1 for a sample larger than 200. We should note
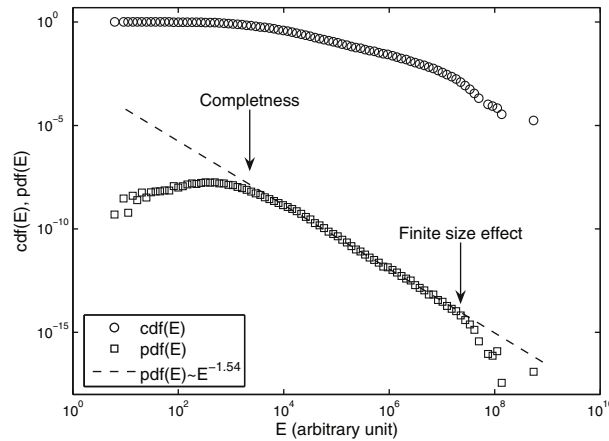
Fig. 2. Earthquake energy distribution of microseismicity induced by mining excavation (courtesy of G. Senfaute, Ineris).

that studies performed in the framework of statistical physics are generally based on several thousand events thus avoiding sampling biases.

The second bias is related to the method used for fitting a power-law trend onto the event size distribution. In the framework of statistical physics, the power-law trend is generally estimated by a linear regression in a log-log plane. When restricted to the power-law trend, this method provides an objective estimation of the exponent giving the same weight to all the size classes, without taking into account the number of events in each class. More elaborate methods combining maximum-likelihood fitting methods with goodness-of-fit tests based on the Kolmogorov-Smirnov statistics have been proposed to estimated both the exponent and the range of the power-law trend [14].

In the field of Earth sciences the maximum likelihood method (MLM) proposed by Utsu and Aki [1,55] is frequently used for estimating the b-value.

$$b = \frac{log_{10}e}{\langle M \rangle - M_{min}}. \tag{8}$$

Where $\langle M \rangle$ and M_{min} are the arithmetic mean and the minimum magnitude of the catalogue. As it uses the mean magnitude, this method provides an estimate controlled essentially by smallest events, i.e. the most numerous. Hence it is less sensitive to the occurrence of largest events than the least squares method. The essential assumption for the validity of the MLM estimate is that M_{min} is above the completeness magnitude [59] (i.e. the magnitude above which the events are detected without sampling biases e.g. regarding the distance to sensors), and that a power-law trend is observed in the full range of magnitudes. In the case where a cut-off exists for the largest events (e.g. in Fig. 2), this method leads to an underestimation of the b-value. The MLM is often associated with the so-called Utsu's test [56] for determining if the difference in b-value observed between two samples is significant. Recently authors [8] used statistical tests to compare least squares and maximum likelihood methods on both natural and synthetic catalogues for estimating biases related to the sampling. They concluded that the Utsu's test gives a biased indication of the significance of a difference in b-value between two catalogues. In particular for small size samples, this test provides a too easy acceptance of the difference as significant. They considered that many previous studies associated the Utsu's test with catalogues of insufficient numbers of events, leading erroneously to consider

insignificant variations of the *b*-value to be significant. According to their study, a sample size of 500 events is the minimum for identifying variations in *b*-value of about 0.1 with a good statistical reliability.

A third bias can exist when comparing cumulative (*cdf*) and discrete (*pdf*) event size distributions. In the case of a *pdf* following a pure power-law, the integration preserves the power-law shape with an exponent shifted by −1 (see Eqs. (1) and (2)). To be correct the *pdf* must be calculated by dividing the number of events in each bin by the bin width. Thus the *pdf* is independent of the binning, whether log or linearly spaced. A potential problem may arise when calculating the *pdf* for magnitude frequency and referring to the Gutenberg-Richter law (Eq. (6)). As the Gutenberg-Richter law corresponds to a linear trend in a semilog plot, the corresponding *cdf* is often calculated with a linearly spaced binning of the magnitude. Because the bin width, measured in magnitude, is constant, the division by the bin width preserve the *b*-value (see Fig. 1). If the comparison between *pdf* and *cdf* is necessary, this problem can be avoided by converting magnitude into energy using Eq. (7) and treating the frequency distribution as a power-law. Figure 1 presents an illustration of the difference between cumulative or discrete distribution for either Magnitude or Energy. For Magnitudes the distribution are expressed in event number ($N(> M)$ and $N(M)$ respectively) respecting the usage in Earth Science (e.g. [45]). It appears clearly that for magnitude the *b*-value is the same for the cumulative and discrete distributions. On the contrary, for the Energy the difference of -1 between the exponents of the *cdf* and the *pdf* is respected.

In the case where a discrepancy with a power-law appears, e.g. cut-off due to the lack of largest events, the integration induces a curvature in the whole distribution that can mask the real power-law segment. This can be seen on Fig. 2 where the power-law trend of the *pdf* appears only between the completeness level, for smallest events, and the cut-off, for largest event ($10^3 > E > 10^8$). These two limits of the power-law trend appear less clearly on the *cdf* and are shifted toward smaller values. The *pdf* is preferable in such a case to avoid associated errors in the estimation of the power-law range.

2.3.2 Finite size effect

The emergence of a pure power-law (i.e. without cut-off) is theoretically possible only within a system of infinite size. In natural conditions such a hypothesis is obviously not found to be true, even if in some cases (e.g. for the whole Earth's crust) the size is large enough to be considered as infinite. In the case of a finite size system, the occurrence of the largest events is constrained by the size of the system. As a consequence the power-law distribution is affected by a exponential tail. Thus the Eq. (2) describing the *pdf* (or Eq. (1) if the *cdf* is considered) should be modified for taking into account the cut-off, e.g. using an exponential decay".

$$p(s) \propto s^{-\beta-1} \exp(-s/s_0) \tag{9}$$

Where s is the size of the event and s_0 is the cut-off size. It has been proposed that the cut-off size s_0 scales with the size of the system L obeying a power law $s_0 \propto L^\delta$ [2,17,49]. The value of exponent δ depends on the dimensionality and on the dynamics of the system. It can be easily determined in the case of numerical simulations by changing the system size L and analysing the size dependence of s_0. In the case of natural systems, the identification of the finite size effect is more difficult as it can be confused with the cut-off related to divergence towards the failure (see Sect. 2.3.3) or the one related to the finite loading rate (see Sect. 1). Mining-induced seismicity provides a good example of cut-off probably induced by finite size effect

of by finite loading rate. In particular if the data set includes all the events related to the collapse process, the effect of distance to the failure can be excluded (see the Sect. 2.3.3). Figure 2 presents microseimic events recorded in a French coal mine (see [47] for more details) for all events recorded during the excavation process up to and including the final rupture induced by the mine collapse. According to the critical behavior expected for this type of brittle failure process, the distribution of the whole catalogue should obey a pure power-law [49]. The cut-off for largest events is more likely to be due to the finite size of the mine that can not induce events as large as determined by the extension of the power-law trend. Alternatively, the loading induced by the cutting at the front of the excavation can be considered as fast enough for activating viscous dissipation inducing a cut-off related to finite loading rate [36,39].

2.3.3 Proximity of failure

Since the work of Scholz [42], the applied stress is the main factor evoked for explaining the change in b-value. This is based on the common laboratory observation where the increase of the applied stress is accompanied by the b-value decrease [3,18,27,31,42], the minimal value being reached just before the macrofailure. This dependency has been used as a proxy for estimating the stress in the Earth's crust, in particular in studies analysing the spatial variability of the b-value [16,34,44,54,60,61].

Considering that the b-value decreases before the macro-failure, several authors have used this parameter for forecasting failure events in natural conditions [7,48, 53,57,58]. In the case of objects for which the macrofailure can be defined clearly, e.g. landslides, cliffs or volcanoes, this approach is relevant as the collapse can be considered as the end of the progressive failure process. More problematic is the case of earthquakes that can be instead considered as part of a marginally stable process that never ends. Here the analysis needs to distinguish the macro-events, i.e. the so-called characteristic earthquakes, from the background seismic activity [53]. The Gutenberg-Richter law, when faithfully respected, contradicts this distinction as no breakdown appears in the scaling law. So there is no reason to distinguish events of a particular size. Alternatively, if a characteristic size appears in the magnitude distribution, the former approach could make sense. The case of the California catalogue presented in Fig. 1 provides a possible application of such separation between large and small events as a characteristic size appears on the magnitude distribution for M larger than 6. We calculated the b-value for successive earthquakes sequences occurring in California in the 1990–2010 period (117100 events). We used a sufficiently large number of events (1000) contained in moving windows to allow a robust estimate of the b-value regarding the sampling bias. Figure 3 shows that significant temporal variations of the b-value exist. In order to verify if this decrease may be considered as a forerunner of large earthquakes, we identify the largest events considering different magnitude thresholds (M>7, M>6, M>5.5). One may first observe that the three M>7 events are preceded by a substantial decrease of the b-value. This could be considered as a promising result as the rate of detection is good. But several times there is a decrease of the b-value without the occurrence of such a large event so that the rate of false alarms is not negligeable. When decreasing the threshold for large events to M>6, the rate of false alarms decreases but the rate of detection too. This effect is enhanced when considering events of M>5.5. The rate of detection failure and false alarms is so high that the forecast ability of the b-value decrease becomes doubtful. An interesting point is that the magnitude distribution (Fig. 1) for events larger than M = 6, displays a slight discrepancy compared to the power-law. So that these larger events could be considered as characteristic earthquakes. This could
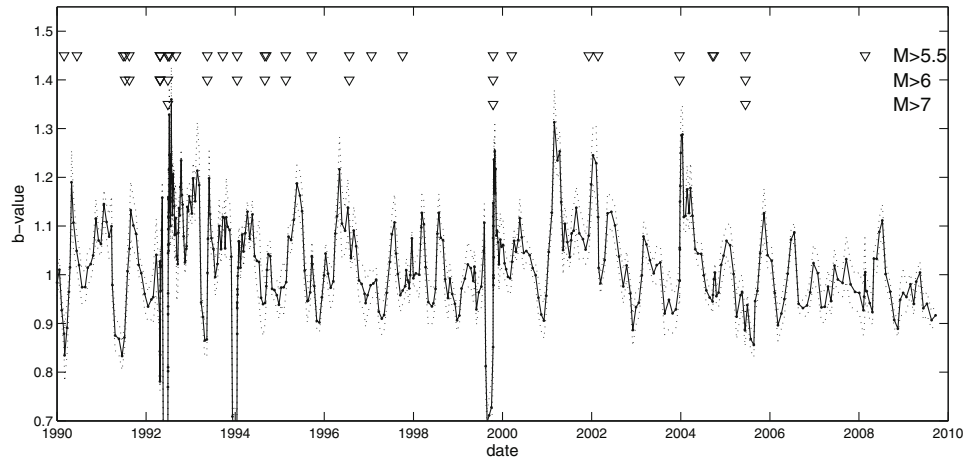
Fig. 3. Temporal evolution of the *b*-value calculated for successive windows of 1000 events with an overlap of 500 events, in California from 1990 to 2010. The 95% confidence interval is given by dotted lines. The catalog includes 117100 earthquakes ranging from M = 2 to M = 7.3. The *b*-value is estimated for the range M = 2 to M = 5 by least square regression. Maximum likelihood method gives comparable results. Triangles indicates the occurrence time for earthquakes larger than magnitude 5.5, 6 and 7.

explain why a precursory behavior appears before these events, but does not explain the occurrence of false alarms. The observed decrease of the *b*-value before large events has been alternatively explained by epidemic models showing that foreshocks, with decreasing *b*-value, can result from cascades of triggered earthquakes [21]. But the characteristic size we observe is not explained by this kind of model.

The stress applied on the material has been early proposed to be an explanative parameter for the *b*-value decrease observed before the failure [42]. Indeed the failure occurs when the stress is increased up to the strength of the material. So the stress has been considered as a measure of the remaining distance before the failure. The absolute value of the material strength may vary strongly depending on the considered material. Therefore for allowing comparisons between various materials, the absolute value of the stress should be normalized by the strength (i.e. the stress value at failure) of each material. The critical point theory rationalizes this statement by defining a control parameter normalizing the distance to the failure. The event size distribution can be expressed as a function of the size s and of the control parameter Δ.

$$p(s,\Delta) \propto s^{-\tau} \cdot \exp(-s/s_0) \qquad (10)$$

With $\Delta = \frac{\sigma_c - \sigma}{\sigma_c}$ for stress controlled loading or $\Delta = \frac{\epsilon_c - \epsilon}{\epsilon_c}$ for strain controlled loading. σ_c and ϵ_c are the stress and strain at the critical point, i.e. the macro-failure. In this description, power-law distribution of the rupture events is associated with an exponential cut-off. According to the critical point theory, the cut-off should diverge when approaching the critical point, whereas the τ exponent should remain constant. The cut-off s_0 divergence when $\Delta \to 0$ has been proposed to be well described by a power law $s_0 \propto \Delta^{-\gamma}$ [2,17,49, Chap. 9].

Including the exponential tail in the range used for fitting the power-law trend, as Δ decreases, could display an apparent decrease of the exponent (see e.g. [7]). This could be the origin of the numerous observations of the apparent *b*-value decrease before the failure. Considering the mechanism of *sweeping an instability*, Sornette [50] has analytically demonstrated that the distribution of the whole population of

events, i.e. including the progressive evolution of the control parameter toward zero, obeys a power-law conforming to the Eq. (9) (see Sect. 4 for a thorough explanation). In such a case, the cut-off is only related to finite size effect.

2.4 Summary

Summarizing the preceding review, excluding incorrect statistics methods, a few candidates arise for explaining variations of the power-law distribution of rupture events observed in natural conditions, experimental and numerical studies.

- Heterogeneity: based on theoretical considerations of the probability of failure in a heterogeneous material, Mogi [32] has proposed that the b-value should increase as the heterogeneity increases.
- Stress: Scholz [42] has first observed a decrease of the b-value when increasing the stress applied on rock samples.
- Proximity of failure: following the previous statement, the b-value decrease has been considered to be a forerunner of the failure. This behavior has been observed prior to some large failure events but remains controversial for large earthquakes.
- Finite size effect: the size of the largest event is constrained by the finite size of the object concerned by the failure. This has been widely and essentially investigated by numerical models of various size. The finite value of loading rate as also been proposed to induce such a cut-off.
- Divergence of the cut-off toward the failure: the exponential tail of power-law is characterized by a cut-off whose size diverges as the failure approaches, the failure is considered to be a critical point.

The latter two points can lead to a biased estimate of the b-value if the range used for estimating it includes the exponential tail.

In the next section we use numerical modeling to evaluate the pertinence of some of the stated potential explanations for the observed variability of power-laws in failure phenomena. In particular we focus on the effect of mechanical properties and on the proximity of the failure.

3 Numerical modeling of progressive damage

3.1 Model features

The model we use here has demonstrated interesting features for investigating power-law emergence in the progressive failure process [3,5,6,17]. It includes elastic interaction within a heterogeneous material with simple damage rules. It is based on progressive isotropic elastic damage. The effective elastic modulus, E_{eff}, is expressed as a function of the initial modulus E_0 and damage D: $E_{eff} = E_0(1 - D)$. Such a relation works when the considered volume is large compared with the defect size, such as cracks, and then can be considered as a mesoscale relationship. The damage parameter D has been proposed to be related to crack density (see [24] for a review). The simulated material is discretized using a 2D finite element method with plane strain hypothesis. The loading consists of increasing the vertical displacement of the upper model boundary. When the stress in an element exceeds a given damage threshold, its elastic modulus is multiplied by a factor $(1 - D)$, D being constant and small compared to 1 (here we used $D = 0.1$). Because of the elastic interaction, the stress redistribution around a damaged element can induce an avalanche of damages that we call an event. The total number of damaged elements during a single loading step
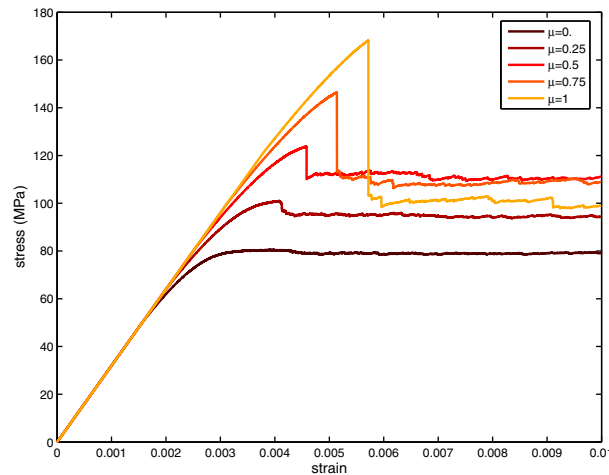
Fig. 4. Macroscopic behavior obtained by numerical simulations for different internal friction values (H = 0.5, μ varies from 0 to 1).

is the avalanche size s, which is comparable to the acoustic emission event amplitude observed in laboratory experiments. The Mohr-Coulomb criterion is used as a damage threshold:

$$\sigma_S = \mu.\sigma_N + C \tag{11}$$

where σ_S is the shear stress; σ_N is the normal stress; C is the cohesion; and μ is the internal friction coefficient. This criterion reflects that the maximum shear stress σ_S the material can sustain increases linearly with the normal stress. Thus it applies well for so-called frictional brittle materials as rocks or ice [23,46]. To obtain macroscopic behaviors differing from those of the elements, damage localization and avalanches size spreading over several magnitude orders, it is necessary to introduce heterogeneity. To simulate material strength heterogeneity, the cohesion of each element, C, is randomly drawn from a uniform distribution. Previous studies have shown that the absolute value of strength doesn't influence the behavior of the model but only changes the scale of the stress/strain relationship. On the opposite, the internal friction μ has a strong influence on the damage localization, the brittle/ductile type of macroscopic behavior and the distribution of avalanches size [5]. Figure 4 shows the macroscopic strain-stress relationship obtained for simulations with internal friction μ ranging from 0 to 1. The macroscopic behavior changes from ductile to brittle, as observed in laboratory experiments for materials characterized by low/high friction. The effect of the friction on the macroscopic behavior has been discussed in depth in previous works [4–6] and has been shown to be related to the interaction geometry between defects that become more anisotropic as the friction increases. This induces a more localized damage (Fig. 5). In the following we focus on the effect of μ on the avalanches distribution.

3.2 Effect of friction on the rupture events size distributions

For the purpose of the present work we carried out simulations with various internal friction values focusing essentially on their impact on the avalanches size distribution. Mechanical parameters have been chosen to correspond to rocks. The used parameters are the following: initial elastic modulus = 50 GPa, Poisson's ratio = 0.25, cohesion
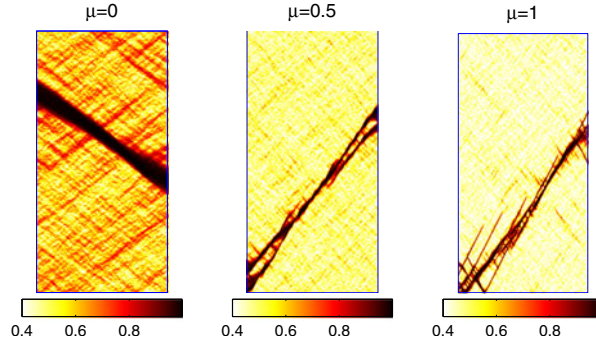
Fig. 5. Damage state of the numerical samples at the end of the simulation, for $\mu = 0$, $\mu = 0.5$, $\mu = 1$.
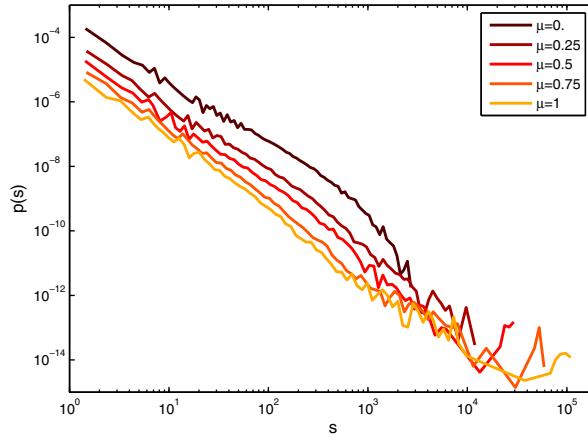

Fig. 6. Event size distribution obtained by numerical simulations for internal friction values μ varying from 0 to 1).

ranging from $C_{min} = 25\,\text{MPa}$ to $C_{max} = 50\,\text{MPa}$, internal friction ranging from 0 to 1. The model size was 128×256 elements. Loading was strain-controlled, i.e. the upper boundary displacement was progressively increased.

Figure 4 shows the macroscopic behavior obtained by numerical simulations with internal friction varying from 0 to 1. The corresponding damage state at the end of the simulation is shown on Fig. 5, for $\mu = 0$, 0.5 and 1 respectively. Increasing the internal friction μ induces a progressive change from ductile to brittle behaviour characterised by the occurrence of a macroscopic stress drop of increasing size. In the case of internal friction very low, i.e. near zero, the stress reaches a metastable value without appearance of a particular point corresponding to the stress peak. So no macro-failure can be individuated in this case. We consider that the macro-failure corresponds to the occurrence of the largest stress drop when it is large enough for affecting significantly the stress-strain curve. In this case it corresponds to the stress peak. The macro-failure associated with the macro-scale stress drop is considered as a critical point in the following.

Regarding the events size distribution including the whole simulation (Fig. 6), one may observe that the internal friction influences both the exponent (β in Eq. (9)) of the power-law trend and the tail shape. The exponent increases with the friction, whereas the tail shape progressively evolves from a cut-off, i.e. lack of large events,

Table 1. Exponents characterizing the event size distribution for various internal friction μ determined from numerical simulations outcomes. β is the exponent characterising the size distribution of the whole set of events during the simulation. R is the oversizing ratio as defined in Sect. 3.2. τ and γ are the exponents characterizing the critical behavior toward the failure (see Eq. (10)). $\tau - 1 + 1/\gamma$ is given for comparison with β.

μ	β ± 0.05	R	τ ± 0.05	γ ± 0.1	$\tau - 1 + 1/\gamma$ ± 0.15
0	0.85	0.004	–	–	–
0.25	0.95	0.055	1.4	2.5	0.8
0.5	1	1.06	1.45	1.7	0.95
0.75	1.2	8.7	1.55	1.6	1.15
1	1.3	20.9	1.6	1.3	1.3

to an oversizing, i.e. occurrence of extreme events out of scale. Hence the macro-failure event generally does not scale with the power-law trend. It is over- or under-estimated depending on the ductile/brittle type of behaviour. In order to characterise the discrepancy between the maximum event size extrapolated from the power-law trend and that occurring during the simulation, we calculated the ratio $R = \frac{max(s_{obs.})}{max(s_{PL})}$, $max(s_{obs.})$ being the maximal observed size during the simulation and $max(s_{PL})$ being the maximal size estimated by the power-law considering the same probability of occurrence. Table 1 shows the values of β and R obtained for the different values of μ. β slightly depends on μ which could explain spatial variations of the b-value observed for earthquakes. More pronounced is the impact of μ on R that varies from values smaller than 1, corresponding to a cut-off, to values larger than 1, corresponding to extreme event compared with the power-law trend. Only in the case of $\mu = 0.5$, does the power-law trend provide a good estimate of the maximum event size, as R is close to 1. An interesting point is that the mean value of friction for the Earth's crust material is estimated to be in the range 0.5–0.6 for seismogenic conditions [12], including the former value. This could explain why cut-off or oversizing are rarely observed for earthquakes. To this concern, earthquakes can be considered as predictable in size.

3.3 Critical behavior toward the failure

In order to characterize how the events size distribution evolves toward the macro-failure, we calculated $p(s)$ for successive bins of the control parameter Δ. As the simulation are realized under strain control condition, $\Delta = \frac{\epsilon_c - \epsilon}{\epsilon_c}$, ϵ_c being the strain at the macro-failure. The binning has been equally spaced in a log scale and sized for ensuring a large enough number of avalanches in each bin. For each bin the representative value of the control parameter has been calculated as the center of the bin in a log scale. For ensuring good statistical representativity we stacked 20 simulations for each configuration. Figure 7 shows the distribution obtained for different values of Δ in the case $\mu = 0.5$. One can observe that the distributions are affected by a cut-off whose size increases with decreasing control parameter. The power-law trend appears fully only for the smallest value of Δ. The τ exponent (see Eq. (10)) has been estimated for the smallest value of the control parameter Δ to be 1.5 ± 0.05. In order to characterize the evolution of the cut-off on approaching the failure, we performed a data collapse conforming to Eq. (10). The best collapse has been obtained for $\tau = 1.45 \pm 0.05$ and $\gamma = 2 \pm 0.1$. We realized the same data collapse for simulations performed with different values of the internal friction. We excluded the value
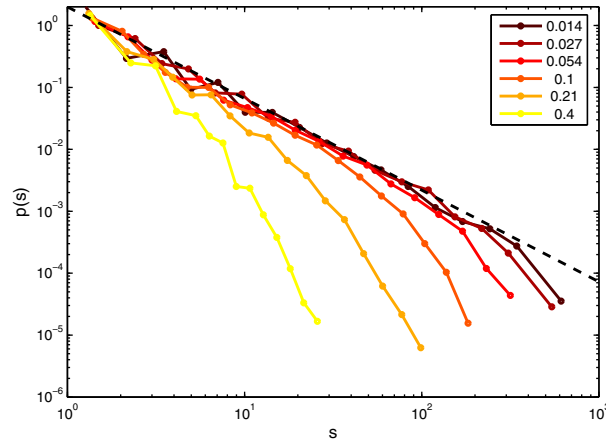
Fig. 7. Event size distribution obtained by numerical simulations for different range of control parameter Δ (indicated in the legend). Simulations have been realized with $\mu = 0.5$. The dotted guide line corresponds to an exponent $-\tau - 1 = -1.5$.
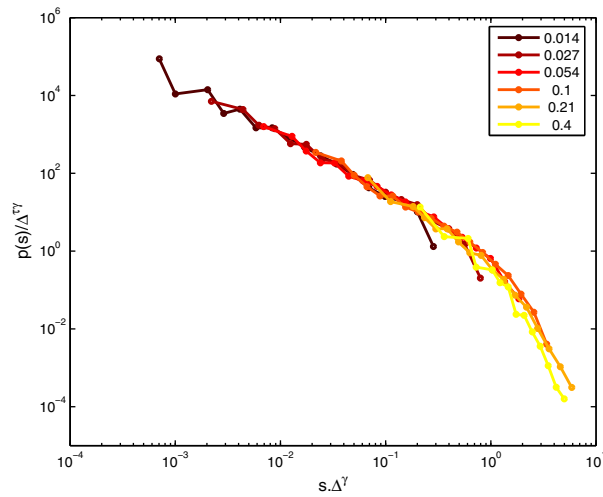

Fig. 8. Data collapse of the probability distributions of event size s for different values of the control parameter (indicated in the legend). The best collapse is obtained with $\gamma = 1.7 \pm 0.1$ and $\tau = 1.45 \pm 0.05$.

$\mu = 0$ as no macroscopic failure can be distinguished on the strain-stress curve for this value (see Fig. 4) so no critical point can be defined. The values of the exponents resulting from this analysis are summarised in Table 1. We observed a slight change for the τ exponent, ranging from 1.4 to 1.55. The impact is more pronounced for the γ exponent, as it varies from 2.5 to 1.3.

This demonstrates the good agreement between the simulations results and the critical point theory. Accordingly the change of events size distribution toward the failure can be fully explained by the divergence of the cut-off as the the failure is approached. But this behavior can be confused with a decrease of the τ exponent if the exponential tail is included in the estimation of the exponent. The discrepancy with the often observed decrease of the b-value, at least for natural objects, may originate in methodological biases. The analysis we developed requires a large number of events,

especially near the failure. This can be difficult to obtain in natural conditions. In the case of catalogues of limited size (i.e. a few hundreds) the identification of the exponential tail can be hard to achieve (e.g. [7]). Moreover, this kind of analysis requires the definition of a well identified control parameter. In the case of natural objects, the control parameter can be difficult to define as the failure may occur under conditions mixing strain and stress (e.g. for crustal earthquakes) or under constant stress (e.g. static fatigue for landslides or rock collapse). When focusing on the short period prior to the failure, the power-law fit provides directly an estimate of the τ exponent (see Fig. 7). In our analyze we observed that this exponent is slightly dependent on the mechanical properties of the material. This could explain the spatial variations of the b-value observed in numerous studies by variations of material properties, when focusing on events occurring just before the macro-failure.

4 Discussion and conclusion

We first reviewed observations showing that a large variability exists in the size distribution of rupture events. Many of these reports concern natural observations of earthquakes, at different scales and in different conditions, and acoustic emissions recorded at the laboratory. The variability concerns essentially the power-law exponent that has been observed to decrease before the failure, essentially at the laboratory but also before some large earthquakes. Spatial variability of the exponent has been also observed. This has been interpreted as the result of variation of either the material properties, as friction and heterogeneity, or of stress. Some rare studies also stated variations in the tail shape identifying either cut-off or oversizing. Besides possible methodological biases, a few potential explanations raised from this review for explaining the observed variability of power-laws.

Theoretical considerations referring to both *critical point theory* [2] and *sweeping of an instability* [50] leads to consider that the events size distribution of the rupture event should be fully described using three exponents instead of a single one. The b-value referring to the Gutenberg-Richter law could be related to different theoretical exponents depending on how it is calculated.

Critical point theory refers to two exponents τ and γ describing the power-law distribution and the divergence of the cut-off size toward the failure, respectively. These two exponents as supposed to be constant for a given material and loading mode. The b-value could be related to the exponent τ only in the vicinity of failure when the value of the exponential tail becomes large enough to not alter the real power-law trend. The decrease of the b-value often observed before the failure should be then considered as an artifact related to the exponential tail of increasing size that is included in the power-law fit. However this apparent decrease provides precursory patterns before the failure useful for the risk assessment. The numerical simulations carried out in Sect. 3 have shown that τ and γ could depend on the mechanical properties of the material. In particular we displayed the effect of the internal friction that controls the brittleness of the macroscopic behaviour.

The mechanism of sweeping of an instability [50] allows to explain that summing the entire set of events of the progressive failure sequence, i.e. including the complete divergence of the exponential cut-off, a power-law distribution is recovered conforming to Eq. (1) or (9), with the relation $\beta = \tau - 1 + 1/\gamma$ (note that the term -1 comes from the fact that β is related to the *cdf*, contrarily to the original work of [50]). The former relation is well respected by the exponents estimated for numerical simulations (see Table 1). Thus, when considering a large set of events including a notable variation of the control parameter (e.g. a long temporal serie of earthquakes or the full set of AE events recorded during an experiment) the b-value can be related to the β exponent.

In this case, the numerical simulation outcomes showed that the β exponent depends also on the mechanical properties of the considered material. This could explain the spatial variations of the b-value observed in different sites (e.g. [60]) and also the variability of the β observed at the laboratory (e.g. [36]).

Moreover, the simulations displayed a dependence between the β exponent and the brittleness of the behaviour. The change in β is associated with a shift from a cut-off to an oversizing characterized by the occurrence of extreme events. The intermediary case for which it is possible to forecast the largest event using the power-law trend of the smallest ones is obtained for $\mu = 0.5$ what corresponds roughly to the mean friction value for the Earth's crust. This suggests that earthquakes could be in the range of predictable events in size. For high internal friction corresponding to highly brittle behavior the largest event, i.e. the size of the macro-failure, is out of scale compared with the power-law trend, we characterized by a high value of the R ratio. Referring to the topic of this special issue, the ductile-brittle transition could be considered as the progressive appearance of Dragon-Kings, i.e. extreme events. Despite their unpredictability in size, considering they obey the critical point theory, these particular events remain predictable in time, at least if a temporal evolution of the control parameter is known, as they emerge from the divergence of the failure process.

References

1. K. Aki, Bull. Earthquake Re. Inst. **43**, 237 (1965)
2. M.J. Alava, P.K.V.V. Nukala, S. Zapperi, Adv. Phys. **55**, 349 (2006)
3. D. Amitrano, J. Geophys. Res. **108** 2044 (2003)
4. D. Amitrano, CR Geosc. **336**, 505 (2004)
5. D. Amitrano, Int. J. Fract. **139**, 369 (2006)
6. D. Amitrano, J.R. Grasso, D. Hantz, Geophys. Res. Lett. **26**, 2109 (1999)
7. D. Amitrano, J.R. Grasso, G. Senfaute, Geophys. Res. Lett. **32**, L08314 (2005)
8. D. Amorese, J.R. Grasso, P.A. Rydelek, Geophys. J. Int. **180**, 347 (2010)
9. Y. Ben-Zion, Rev. Geophys. **46**, RG4006 (2008)
10. R. Bossu, J.R. Grasso, L.M. Plotnikova, B. Nurtaev, J. Frechet, M. Moisy, Bull. Seismol. Soc. Amer. **86**, 959 (1996)
11. R. Burridge, L. Knopoff, Bull. Seismol. Soc. Amer. **57**, 341 (1967)
12. J.D. Byerlee, Pageoph **116**, 615 (1978)
13. K. Chen, P. Bak, S.P. Obukhov, Phys. Rev. A **43**, 625 (1991)
14. Aaron Clauset, Cosma Rohilla Shalizi, M.E.J. Newman, SIAM Rev. **51**, 661 (2009)
15. K.A. Dahmen, Y. Ben-Zion, J.T. Uhl, **102**, 175501 (2009)
16. M. Gerstenberger, S. Wiemer, D. Giardini, Geophys. Res. Lett. **28**, 57 (2001)
17. L. Girard, D. Amitrano, J. Weiss, J. Stat. Mech. **P01013**, (2010)
18. A. Guarino, A. Garcimartin, S. Ciliberto, Eur. Phys. J. B **6**, 13 (1998)
19. B. Gutenberg, C.F. Richter, *Seismicity of the Earth and Associated Phenomena* (Princeton University Press, Princeton, 1954)
20. Thomas C. Hanks, Hiroo Kanamori, J. Geophys. Res. **84**, 2348 (1979)
21. A. Helmstetter, D. Sornette, J. Geophys. Res. **108**, 2457 (2003)
22. T. Hirata, T. Satoh, K. Ito, Geophys. J. R. Astr. Soc. **90**, 369 (1987)
23. J.C. Jaeger, N.G.W. Cook, *Fundamentals of Rock Mechanics* (Chapman and Hall, London, 1979)

24. J. Kemeny, N.G.W. Cook, Int. J. Rock Mech. Min. Sci. Geomech. Abstr. **23**, 107 (1986)
25. X. Lei, K. Masuda, O. Nishizawa, L. Jouniaux, L. Liu, W. Ma, T. Satoh, K. Kusunose, J. Struct. Geol. **26**, 247 (2004)
26. C.H. Lin, Terrestrial Atmosph. Oceanic Sci. **21**, 229 (2010)
27. D.A. Lockner, Int. J. Rock Mech. Min. Sci. Geomech. Abstr. **30**, 883 (1993)
28. D.A. Lockner, J.D. Byerlee, *Precursory AE Patterns Leading to Rock Fracture*, Vth Conf. AE/MS Geol. Str. Mat., edited by Hardy (The pennsylvania State University) (Trans Tech Publication, Germany, 1991), p. 45
29. I. Main, Bull. Seismol. Soc. Amer. **90**, 86 (2000)
30. M. Mekkawi, J.-R. Grasso, P.A. Schnegg, Bull. Seismol. Soc. Amer. **94**, 479 (2004)
31. P.G. Meredith, I.G. Main, C. Jones, Tectonophysics **175**, 249 (1990)
32. K. Mogi, Bull. Earthquake Res. Inst. Univ. Tokyo **40**, 831 (1962)
33. C. Montuori, G. Falcone, M. Murru, C. Thurber, M. Reyners, D. Eberhart-Phillips, Geophys. J. Int. **183**, 451 (2010)
34. J. Mori, R.E. Abercombie, J. Geophys. Res. **102**, 15081 (1997)
35. Z. Olami, H.J.S. Feder, K. Christensen, Phys. Rev. Lett. **68**, 1244 (1992)
36. C.B. Picallo, J.M. Lopez, Phys. Rev. E **77**, 046114 (2008)
37. G. Pickering, J.M. Bull, D.J. Sanderson, Tectonophysics **248**, 1 (1995)
38. S. Pradhan, P. Bhattacharyya, B.K. Chakrabarti, Phys. Rev. E **66**, 016116 (2002)
39. A. Rosso, A.K. Hartmann, W. Krauth, Phys. Rev. E **67**, 021602 (2003)
40. J. Rostil, J. Koivisto, M. Alava, J. Stat. Mech.: Theory Exper. **2010**, P02016 (2010)
41. P. Sammonds, M. Ohnaka, Geophys. Res. Lett. **25**, 699 (1998)
42. C.H. Scholz, Bull. Seismol. Soc. Amer. **58**, 399 (1968)
43. C.H. Scholz, *The Mechanics of Earthquakes and Faulting* (Cambridge University Press, 1990)
44. D. Schorlemmer, S. Wiemer, Nature **434**, 1086 (2005)
45. D. Schorlemmer, S. Wiemer, M. Wyss, Nature **437**, 539 (2005)
46. E.M. Schulson, D. Illiescu, C.E. Renshaw, J. Geophys. Res. **104**, 695 (1999)
47. G. Senfaute, C. Chambon, P. Bigarre, Y. Guise, J.P. Josien, Pageoph **150**, 451 (1997)
48. W.D. Smith, Nature **289**, 136 (1981)
49. D. Sornette, *Critical phenomena in Natural Sciences, Chaos, Fractals, Self Organization and Disorder: Concepts and Tools* (Berlin, New-York, 2000)
50. D. Sornette, J. Phys. I (France) **4**, 13 (1994)
51. C. Sue, J.R. Grasso, F. Lahaie, D. Amitrano, Geophys. Res. Lett. (France) **29**, 65 (2002)
52. C.A. Tang, Int. J. Rock Mech. Min. Sci. Geomech. Abstr. **34**, 249 (1997)
53. Y. Tsukakoshi, K. Shimazaki, Earth Planets Space **60**, 915 (2008)
54. T.I. Urbancic, C.I. Trifu, J.M. Long, R.P. Young, Pageoph **139**, 449 (2008)
55. T. Utsu, Geophys. Bull. Hokkaido Univ. **13**, 99 (1965)
56. T. Utsu, J. Phys. Earth **14**, 37 (1966)
57. S. Vinciguerra, J. Volcanol. Geoth. Res. **2383**, 1 (2002)
58. S. Vinciguerra, S. Gresta, M.S. Barbano, G. Distefano, Geophys. Res. Lett. **28**, 2257 (2001)
59. S. Wiemer, M. Wyss, Bull. Seismol. Soc. Amer. **90**, 859 (2000)
60. S. Wiemer, M. Wyss, Adv. Geophys. **45**, 259 (2002)
61. M. Wyss, K. Shimazaki, S. Wiemer, J. Geophys. Res. **102**, 20413 (1997)
62. S. Zapperi, P. Nukala, Int. J. Fract. **140**, 99 (2006)
63. S. Zapperi, A. Vespignani, E. Stanley, Nature **388**, 658 (1997)